University of Massachusetts - Amherst
ScholarWorks@UMass Amherst

Mathematics and Statistics Department Faculty Publication Series

Mathematics and Statistics

2010

Stable structures with high topological charge in nonlinear photonic quasicrystals

K Law

A Saxena

PG Kevrekidis
University of Massachusetts - Amherst, kevrekid@math.umass.edu

Follow this and additional works at: http://scholarworks.umass.edu/math_faculty_pubs

Part of the Physical Sciences and Mathematics Commons

Law, K; Saxena, A; and Kevrekidis, PG, "Stable structures with high topological charge in nonlinear photonic quasicrystals" (2010). *Mathematics and Statistics Department Faculty Publication Series.* Paper 1065.
http://scholarworks.umass.edu/math_faculty_pubs/1065

This Article is brought to you for free and open access by the Mathematics and Statistics at ScholarWorks@UMass Amherst. It has been accepted for inclusion in Mathematics and Statistics Department Faculty Publication Series by an authorized administrator of ScholarWorks@UMass Amherst. For more information, please contact scholarworks@library.umass.edu.

Stable structures with high topological charge in nonlinear photonic quasicrystals

K. J. H. Law,[1,2] Avadh Saxena,[3] P. G. Kevrekidis,[2] and A. R. Bishop[3]

[1] *Warwick Mathematics Institute, University of Warwick, Coventry CV4 7AL, UK*
[2] *Department of Mathematics and Statistics, University of Massachusetts, Amherst MA 01003-4515, USA*
[3] *Theoretical Division and Center for Nonlinear Studies, Los Alamos National Laboratory, Los Alamos, NM 87545, USA*

Stable vortices with topological charge of 3 and 4 are examined numerically and analytically in photonic quasicrystals created by interference of 5 as well as 8 beams, for cubic as well as saturable nonlinearities . Direct numerical simulations corroborate the analytical and numerical linear stability analysis predictions for such experimentally realizable structures.

PACS numbers: 42.65.Tg, 03.75.Lm, 61.44.Br, 63.20.Pw

arXiv:1003.2779v2 [nlin.PS] 17 Jul 2010

Introduction. The study of vortices has been a principal theme of interest in dispersive nonlinear systems with applications including, among others, Bose-Einstein condensates (BEC), and nonlinear optical media [1–3]. More recently, such states have been studied in settings with some discrete spatial symmetry i.e., nonlinear lattices. There, the notion of "discrete vortices" [4] arose and was subsequently intensely studied in both discrete and quasi-continuum media; see e.g. [5, 6] for relevant reviews. This led to the experimental realization of unit-charge ($S = 1$) coherent structures in saturably nonlinear photorefractive media [such as SBN:75($Sr_0.75Ba_0.25Nb_2O_6$)] in [7, 8], and the exploration of higher charge ($S = 2$) ones in square and hexagonal/honeycomb lattice settings [9]. A multipole soliton necklace of out-of-phase neighboring lobes in a square lattice was identified experimentally and theoretically in [10] from initial condition of a wide $S = 4$ gaussian beam.

While regular lattices have been mostly studied [5], more recently experimental developments have enabled the study of photonic quasicrystals in photorefractive media [11], and have spurred a correspondingly intense theoretical activity [12]. We also note that recent experiments have emerged on non-square optical lattices for ultracold atoms in the BEC case [13]. It is then natural to expect that quasi-crystals are well within experimental reach in this regard, as well.

Motivated by these developments, we illustrate the unique ability of such lattices (with saturable or cubic nonlinearity) to sustain stable vortices of higher topological charge, such as $S = 3$ and $S = 4$. Direct numerical simulations reveal the robustness of such modes. On the other hand, perhaps counter-intuitively (but as can be analytically predicted), lower charge vortices are found to be unstable, and this instability is also dynamically monitored.

Theoretical Setup. We introduce the following non-dimensionalized evolution equation:

$$\left[i\partial_z + \frac{1}{2}\nabla^2 + F(|U|^2) - V(\mathbf{x})\right] U = 0. \qquad (1)$$

The (saturable) photorefractive nonlinearity is $F(|U|^2) = -1/(1 + |U|^2) + 1$, where U is the slowly varying amplitude of a probe beam normalized by the dark irradiance of the crystal I_d [3, 14], and V represents modulation of the refractive index from interfering linearly propagating waves normal to the probe beam. In a Kerr medium the nonlinearity reads $F(|U|^2) = |U|^2$, and this case also includes the interpretation of U as a mean-field wavefunction of an atomic Bose-Einstein condensate [15], while the potential V is either modulation of the refractive index in the former case or an externally applied field in the latter.

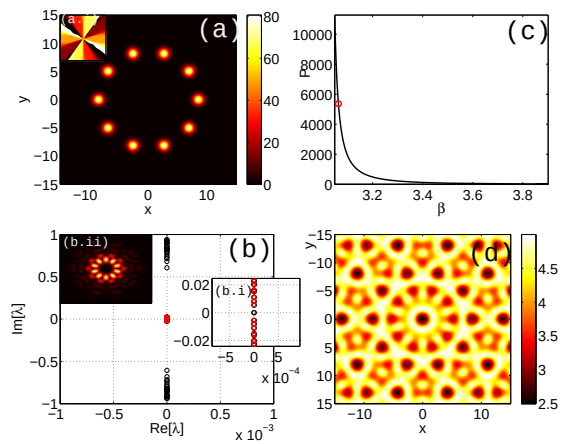

FIG. 1: (Color online) The stable $S = 4$ vortex in a quasi-crystal lattice of $N = 5$ and with a saturable nonlinearity. The profile and phase are depicted in panels [a(.i)], the linear spectrum in panel (b), Fourier spectrum in the inset panel (b.i), and continuation of the power, $P = \int |U|^2 d\mathbf{x}$, as a function of the propagation constant, β, in panel (c). The $N = 5$ lattice is depicted in (d).

The potential V is taken to be of the form $E/(1+I(x))$, where $I(\mathbf{x}) = \frac{1}{N^2}\left|\sum_{j=1}^{N} e^{ik\mathbf{b}_j\cdot\mathbf{x}}\right|^2$. In the photorefractive paradigm, this is the optical lattice intensity function formed by N interfering beams in the principal directions $\mathbf{b}_j$ with periodicity $2\pi/k$. We will consider the cases of

$N = 5$ and $N = 8$. Here 1 is the lattice peak intensity, z is the propagation constant, $\mathbf{x} = (x, y)$ are transverse distances, $k = 2\pi/5$ is the wavenumber of the lattice, and $E = 5$ is proportional to the external voltage. Recently, such a setting has been explored theoretically for positive lattice solitons [12, 16], but we extend the considerations here to vortex solutions.

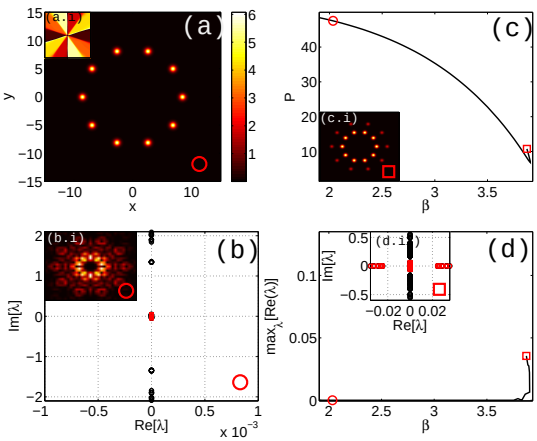

FIG. 2: (Color online) Panels (a-c) are the same as Fig. 1 except for a cubic nonlinearity. Panel (d) shows the growth rate, or $\max_\lambda[Re(\lambda)]$. The insets, (c.i) and (d.i) depict the profile and linear spectra, respectively, of the highly unstable solution indicated by a red square on the branches in (c,d), which collides with the main branch and disappears in a saddle node bifurcation close to the phonon band edge.

The possible charge, S, of vortices (the number of 2π phase shifts across a discrete contour comprising the solution) is bounded by the symmetry of the lattice [17]. A lattice with n-fold symmetry has natural contours of $2n$ sites. Hence, taking into account the degeneracy of vortex anti-vortex pairs $\{S, -S\}$, one has $0 \leq S \leq n$, with the cases of $S = 0, n$ being the trivial flux cases of in-phase and out-of-phase neighboring lobes, respectively. The quasi-crystal with $N = 5$ has $n = 5$, while for $N = 8$, $n = 4$. Hence, the highest possible charge, $S = n - 1$, is $S = 4$ for the case of $N = 5$ and $S = 3$ for $N = 8$.

Considering the quasi-one-dimensional contour of excited sites (depending on the respective amplitudes of the lattice and the probe field), and within the context of coupled mode theory [18] in which the probe field is expanded in Wannier functions [19], one can obtain insights about the stability of the vortices within the framework of a discrete Nonlinear Schrödinger equation [6], $i\dot{u}_n = -\varepsilon(u_{n+1} + u_{n-1} - 2u_n) - |u_n|^2 u_n$. In that context and based on either the modulational instability of [18], or through empirical numerical testing [17] or, more rigorously, via Lyapunov-Schmidt perturbative expansions around the so-called *anti-continuum* (AC) limit of zero coupling ($\varepsilon = 0$) [20], it is known that lobes which are phase-separated by greater than $\pi/2$ are stable next to each other, while those separated by less than $\pi/2$ are unstable. A simple intuitive argument for this situation is that the effective potential which out-of-phase neighboring nodes exert on one another through the focusing non-linearity is repulsive, and, hence, remain localized in their respective separate wells. On the other hand, if the neighbors are in-phase, then the effective neighboring potentials are attractive and hence the solution is unstable to remaining localized in separate wells. The possible relative phases interpolate between these cases, with $\pi/2$ being exactly in the middle. A similar discussion is used in [21] in order to justify (upon suitable phase variation) the existence of soliton clusters in bulk media. This leads to stability of the *higher* charged vortices for contours of larger numbers of nodes (see also [9]). We briefly review the Lyapunov-Schmidt argument. In the limit $\varepsilon \to 0$ one can construct exact solutions of the form $u_j = \sqrt{\mu} e^{\{-i(\beta t - \theta_j)\}}$ for any arbitrary $\theta_j \in [0, 2\pi)$ [20]. The case we are considering is that of $\theta_j = jS\pi/n$. We linearize around the solution for $\varepsilon = 0$ and the condition for existence of solutions with $\varepsilon > 0$ reduces to the vanishing of a vector function $\mathbf{g}(\boldsymbol{\theta})$ of the phase vector $\boldsymbol{\theta} = (\theta_1, \ldots, \theta_N)$, where

$$g_j \equiv \sin(\theta_{j-1} - \theta_j) + \sin(\theta_{j+1} - \theta_j), \qquad (2)$$

subject to periodic boundary conditions. This includes the discrete reduction of the vortex solutions for $0 \leq S \leq n$ above. The fundamental contours M will have length $|M| = 2n$, and $|\phi_{j+1} - \phi_j| = \Delta\phi = \pi S/n$ is constant for all $j \in M$, $|\theta_1 - \theta_{|M|}| = \Delta\theta$ and $\Delta\theta|M| = 0 \bmod 2\pi$.

For the contour M, there are $|M|$ eigenvalues γ_j of the $|M| \times |M|$ Jacobian $\mathcal{M}_{jk} = \partial g_j/\partial\theta_k$ of the diffeomorphism given in Eq. (2). The eigenvalues of this matrix γ_j can be mapped eigenvalues of the full linearization. In particular, eigenvalues of the linearization, denoted λ_j, are given to leading order by the relation [20] $\lambda_j = \pm\sqrt{2\gamma_j\varepsilon}$. Thus, solutions are stable to leading order if $\gamma_j < 0$ (so $\lambda_j \in i\mathbb{R}$) and unstable if $\gamma_j > 0$ (so $\lambda_j \in \mathbb{R}$). We have $\gamma_j = 4\cos(\Delta\phi)\sin^2\left(\frac{\pi j}{|M|}\right)$ and so these cases correspond exactly to $\Delta\phi > \pi/2$ (or $S > n/2$) and $\Delta\phi < \pi/2$ (or $S < n/2$). In the boundary case of $\Delta\phi = \pi/2$, one needs to expand to the next order in the Lyapunov-Schmidt reduction. We note that a so-called staggering transformation along the contour, $u_j^d = (-1)^j u_j^f$ allows the above conclusions for the focusing problem to be mapped immediately to the defocusing problem (with a change in the sign of the nonlinearity). We do not consider the defocusing case further here. The above considerations illustrate the expectation that $S = 3$ vortices may be stable in the $N = 5$ and $N = 8$ cases, and the $S = 4$ vortex may be stable in the $N = 5$ case.

Numerical Results. We now turn to numerical com-

putations. We also explore the evolution of different S radial gaussian beams.

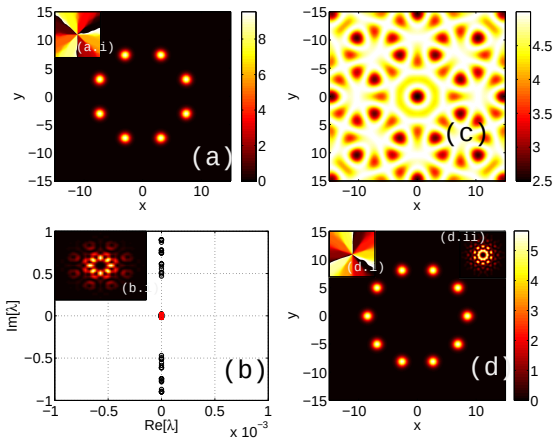

FIG. 3: (Color online) Panels (a,b) are the same as the previous figures for the stable $S = 3$ vortex in the $N = 8$ quasi-crystal lattice (c). Panel (d) is the $S = 3$ vortex for $N = 5$ and [d.(i,ii)] are the phase and Fourier spectrum, respectively, of this solution. For both solutions, $\beta = 3.4$.

First, we confirm the expectation of stability of the $S = 4$ vortex for saturable and cubic nonlinearities, over continuations in the semi-infinite gap (see Figs. 1 and 2, respectively). The profiles and phases are depicted in panels [a(.i)], linear spectra in panels (b), Fourier spectra in the inset panels (b.i), and continuations of the power, $P = \int |U|^2 d\mathbf{x}$, as a function of the propagation constant, β, in panels (c). The power of the solution branches differs substantially between nonlinearities, and the power of the branch of saturable solutions approaches some resonant frequency at which $dP/d\beta \to \infty$ and $P \to \infty$ (see Fig. 1 (c)). The lattice is depicted in Fig. 1 (d), while Fig. 2 (d) shows the maximal perturbation growth rate, or $\max_\lambda[Re(\lambda)]$, corresponding to the branches in Fig. 2 (c).

For the structures we consider, there is one pair of eigenvalues at the origin accounting for the U(1) (phase) invariance and the other $2n - 1$ eigenvalue pairs associated to the excited lobes all have negative energy, hence being candidates for instability [22], and are all either purely imaginary or purely real. If real, the instability is immediate, while if imaginary, instability may still arise due to their collision with the phonon band, resulting in a Hamiltonian-Hopf bifurcation and eigenvalue quartets. The spectral plane, with the negative energy modes indicated by red squares, for the saturable and cubic cases are given in panels (b) of Figs. 1 and 2, respectively. Panel (b.ii) in Fig. 1 is a closeup of the origin showing the 9 negative energy pairs close to the origin and the one pair at the origin. The potential instability arising from these negative energy modes is prevented by their proximity

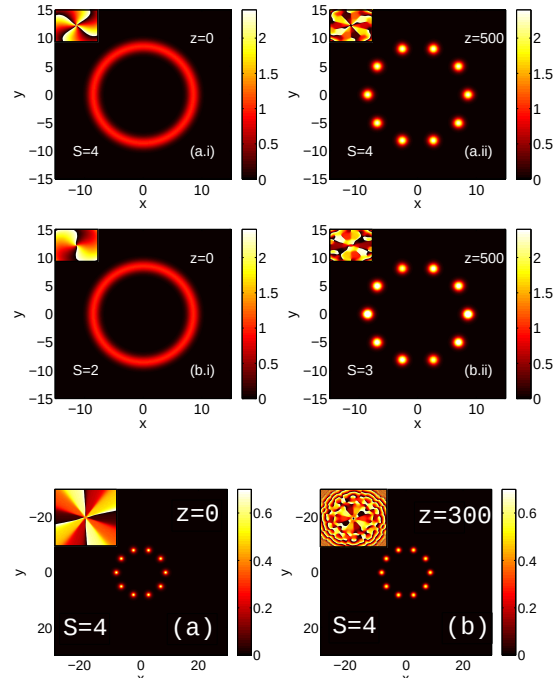

FIG. 4: (Color online) Initial conditions (a.i,b.i) and profiles at a later time (a.ii,b.ii) of the $S = 4$ and $S = 2$ radial Gaussian initial conditions for a saturable nonlinearity, with a "tight dissipation layer" (see text), $D = 16$. The bottom is similar to the top but for $D = 24$.

to the origin, and distance from the phonon band. The expected saddle-node bifurcation [23, 24] occurs close to the band edge (which we computed as ≈ 3.9) in which the main solution collides (and disappears) with an unstable solution branch of a configuration with additional populated sites external (and in phase) to the original contour.

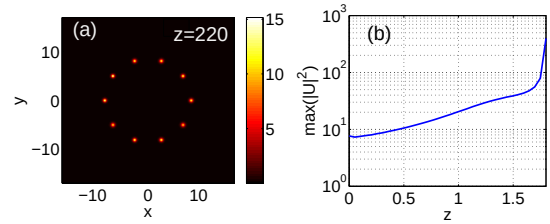

FIG. 5: (Color online) The dynamics of the unstable $S = 2$ vortex in the case of a cubic nonlinearity. Evolution of the same solution with the same perturbation of random noise with 5% of the initial maximum amplitude of the field can lead to robust structures that persist for long distances (a) and almost immediate collapse in different trials (b).

Next, we present results of the $S = 3$ vortex in both the $N = 8$ (Fig. 3(a,b)) and $N = 5$ (Fig. 3 (d)) cases for

$\beta = 3.4$. Panel (c) depicts the $N = 8$ lattice, and [d.(i,ii)] are the phase and Fourier spectrum, respectively, of the solution in (d). These solutions are both stable, and again there is a resonance in the semi-infinite gap (not shown) similar to what was seen in Fig. 1. The vortices for $S < 3$ are unstable (not shown).

To examine the potential experimental realizability of the above waveforms, we launch a radial Gaussian beam with topological charge $S = 4$ of the form $e^{iS\theta-(r-R)^2/(2b^2)}$ with (r, θ) denoting polar coordinates, $R = 8.5$, approximately the radius of the contour, and $b = 1$, as an initial condition into the system with saturable nonlinearity and monitor the evolution. After a transient period, the configuration indeed settles into an $S = 4$ vortex contour. However, notice that this simulation has been performed with a "tight dissipation layer" i.e. using an extra term $-i\Gamma$ on the right-hand side of Eq. 1) of $\Gamma = 1-\tanh(D-\mathbf{r})$ with $D = 16$. This initially absorbs the shed radiation, and subsequently affects very little the intensity distribution. However, the phase dynamics may be sensitive to the presence of such a layer: imposing a wider such dissipation layer with $D = 24$, the solution actually never settles into one of constant charge; this topological instability effect has been analyzed e.g. in [25–28]. Specifically, vortices may nucleate in the very small amplitude region and pass in and out of the main configuration (without affecting its intensity). Note that the above suggests that such effects could be avoided experimentally if some form of dissipation is imposed. For comparison, we launch a similar initial condition with $S = 2$ and notice that it never settles into a stable configuration of fixed charge *independently of the dissipation layer size* (and despite its seemingly robust intensity distribution).

Figure 4 (top two panels) present the initial conditions (a.i,b.i) and profiles for a long evolution (a.ii,b.ii) of the $S = 4$ and $S = 2$ initial conditions, respectively, for saturable nonlinearity and $D = 16$. The charge of each fluctuates, as power is shed and vortices nucleate in the surrounding low amplitude regions and enter and leave the contour as the solution traces a stationary state. However, for the $S = 4$ initial condition, the field settles into a solution of constant charge 4 for $D = 16$, while for the $S = 2$ initial condition, the phase continues to fluctuate throughout the numerical experiment. These results are typical in this setting. For D large (bottom panel of Fig. 4) the charge may never settle (topological phase instability). However, this does not contradict the linear stability results (which we have confirmed separately for near stationary configurations). The intial condition $e^{iS\theta-(r-R)^2/(2b^2)}\cos^2(5\theta)$ is far from a stationary configuration and not sufficiently modulated to prevent contamination of the resulting state by radiation, although e.g. $\sum_{k=1}^{10} e^{ikS\pi/5-(x-c_{xk})^2-(y-c_{yk})^2}$ with (c_{xk}, c_{yk}) the center of one of the wells, is sufficiently localized, and with the latter initial condition, we observe topological stability (indeed without the initial turbulent fluctuating regime) for $S = 4$ (see Fig. 4) but not for $S = 2$. Finally, Fig. 5 shows the evolution of unstable ($S = 2$) vortices in the presence of a cubic nonlinearity. The evolution depends sensitively on the particular initial condition. Using the initial condition $u = U(1+X)$ with $X \sim 0.05\max_{\mathbf{x}}[U(\mathbf{x})]$ uniform over [0,1], two different particular instances can lead to significantly different dynamics. Either the phase merely reshapes as for the saturable nonlinearity, but the structure persists [see Fig. 5 (a)], or the solution collapses almost immediately, as seen from the maximum amplitude of the field in Fig. 5 (b). For larger additive noise, collapse seems more likely from several sample trials. The relevant mechanism involves one of the solution lobes exceeding a minimum collapse threshold, leading to an "in lobe" collapse.

Conclusions and future directions. We have demonstrated numerically stable vortices of topological charge $S = 3$ in quasi-crystals with $n = 4$ and 5 directions of symmetry and $S = 4$ with $n = 5$, in the cases of both cubic and saturable focusing nonlinearities. The negative energy modes for these configurations remain close to the origin in the spectral plane, preventing collision with the phonon band, and can be experimentally realizable in photonic quasi-crystals in a photorefractive (or a Kerr) medium. This has additionally been demonstrated by simulation of the evolution of a radial Gaussian beam into such robust vortex states. This is a prime prospect for an immediate future experimental direction related to the present work.

Acknowledgments. KJHL acknowledges LANL and CNLS for hospitality. The work was supported by NSF and DoE.

[1] L.M. Pismen, *Vortices in Nonlinear Fields*, (Oxford University Press, Oxford, 1999).
[2] A.L. Fetter, Rev. Mod. Phys. **81**, 647 (2009).
[3] Y.S. Kivshar and G.P. Agrawal, *Optical Solitons: From Fibers to Photonic Crystals*, (Academic Press, London, 2003).
[4] B.A. Malomed and P.G. Kevrekidis, Phys. Rev. E **64**, 026601 (2001).
[5] F. Lederer *et al.*, Phys. Rep. **463**, 1 (2008).
[6] P.G. Kevrekidis, *The Discrete Nonlinear Schrödinger Equation*, (Springer-Verlag, Heidelberg, 2009).
[7] D.N. Neshev *et al.*, Phys. Rev. Lett. **92**, 123903 (2004).
[8] J.W. Fleischer *et al.*, Phys. Rev. Lett. **92**, 123904 (2004).
[9] K.J.H. Law *et al.*, Phys. Rev. A **80**, 063817 (2009); B. Terhalle *et al.*, Phys. Rev. A **79**, 043821 (2009).
[10] J. Yang *et al.*, Phys. Rev. Lett. **94**, 113902 (2005).
[11] B. Freedman *et al.*, Nature **440**, 1166 (2006).
[12] M. J. Ablowitz *et al.*, Phys. Rev. E **74**, 035601(R) (2006).
[13] C. Becker *et al.*, New J. Phys. **12**, 065025 (2010).
[14] N.K. Efremidis *et al.*, Phys. Rev. E **66**, 46602 (2002).
[15] L.P. Pitaevskii and S. Stringari, *Bose-Einstein Condensation*, (Oxford University Press, Oxford, 2003).

[16] Y. Sivan, *et al.*, Phys. Rev. E **78**, 046602 (2008).
[17] Y. V. Kartashov, *et al.*, Phys. Rev. Lett. **95**, 123902 (2005).
[18] D.N. Christodoulides and R.I. Joseph, Opt. Lett. **13**, 794 (1988); Yu.S. Kivshar and M. Peyrard, Phys. Rev. A **46**, 3198 (1992).
[19] W. Kohn, Phys. Rev. **115**, 809 (1959).
[20] D.E. Pelinovsky, P.G. Kevrekidis, and D.J. Frantzeskakis, Physica D **212**, 1 (2005); *ibid.* 20 (2005).
[21] A. S. Desyatnikov and Y. S. Kivshar, Phys. Rev. Lett. **88**, 053901 (2002).
[22] J. C. van der Meer, Nonlinearity **3**, 1041 (1990).
[23] J. Wang and J. Yang, Phys. Rev. A. **77**, 033834 (2008).
[24] H. Susanto *et al.*, Physica D **237**, 3123 (2008).
[25] A.S. Desyatnikov, Yu.S. Kivshar and L. Torner, Prog. Optics **47**, 291 (2005).
[26] A. Bezryadina, *et. al.*, Opt. Exp. **14**, 8317 (2006).
[27] B. Terhalle, *et. al.*, Phys. Rev. Lett. **101**, 013903 (2008).
[28] B. Terhalle, *et. al.*, Opt. Lett. **35**, 604 (2010).